ejpmr, 2017,4(05), 325-339

SJIF Impact Factor 4.161

EUROPEAN JOURNAL OF PHARMACEUTICAL AND MEDICAL RESEARCH

www.ejpmr.com

Research Article

ISSN 2394-3211

EJPMR

FORMULATION AND EVALUATION OF COX-2 INHIBITOR LOADED GOLD NANOPARTICLES ENRICHED HYDROGEL FOR TREATMENT OF RHEUMATOID ARTHRITIS.

Jessy Shaji* and Seema Darade

Dept. of Pharmaceutics, Prin. K. M. Kundnani College of Pharmacy, Cuffe Parade, Mumbai 400005, India.

***Corresponding Author: Jessy Shaji**

Dept. of Pharmaceutics, Prin. K. M. Kundnani College of Pharmacy, Cuffe Parade, Mumbai 400005, India.

Article Received on 22/02/2017 **Article Revised on 15/03/2017** **Article Accepted on 05/04/2017**

ABSTRACT

In the present study, we synthesized Piroxicam Monoethanolamine (PRX-MEA) conjugated gold nanoparticles (PM-AuNPs) by a simple economic, nontoxic green synthesis using Camellia sinesis (green tea) extract as reducing agent and Tween 80 as stabilizer. PM-AuNPs were developed using 19 run, 3 factors and 2-level full factorial design. The particle size and zeta potential of the optimized batch were 51.2 ± 33.8 nm and -30.2 ± 14.2 mV respectively. The loading efficiency of PRX-MEA was found to be 89.05 ± 0.41%. The surface morphology of gold nanoparticles was investigated by TEM. The synthesized particles were largely spherical in shape with a smooth morphology. Selected area electron diffraction (SAED) pattern revealed diffraction patterns of crystalline gold structure. FTIR spectroscopy identified the conjugation of PRX-MEA to the surface of AuNPs. The structural characterization and crystalline nature of PM-AuNPs was determined by XRD. Furthermore, in this study PM-AuNPs enriched hydrogel was fabricated and evaluated for pH, drug content and spreadability. PM-AuNPs dispersion and hydrogel were studied for an *in- vitro* drug release and skin permeation potential. The cumulative percentage drug released at the end of 48 h was found to be 91.24 ± 3.48%. In transdermal experiments, the steady state flux and the permeability coefficient of PM-AuNPs and PM-AuNPs hydrogel were significantly higher than plain drug solution ($p<0.01$). In the *in-vitro* antioxidant assay and *in-vivo* anti-inflammatory activity PM-AuNPs showed superior activity over PRX-MEA. The results indicate that the developed formulation offers significant protection towards inflammatory effects in rheumatoid arthritis.

KEYWORDS: Piroxicam monoethanolamine, rheumatoid arthritis, gold nanoparticles, green tea, hydrogel, anti-inflammatory.

INTRODUCTION

Rheumatoid arthritis (RA) is a chronic inflammatory condition of unknown etiology affecting approximately 1% of the general population worldwide.[1] Despite of extensive studies, finding an effective and long lasting therapy, specifically targeted for RA, is still a demanding task.[2] Early treatment of RA with COX-2 inhibitors may induce long term and sustained functional therapeutic effect. They work by reducing the levels of prostaglandins, chemicals that are responsible for pain, fever, and inflammation.[3] Piroxicam results in inhibition of the enzyme COX-2 that makes prostaglandins (cyclooxygenase), leading to lower concentrations of prostaglandins. As a consequence, inflammation, pain and fever are reduced. The FDA approved Piroxicam in 1982, for the relief of rheumatoid arthritis and osteoarthritis. The recommended dose is 20 mg given orally once per day.[4]

Furthermore, the poor pharmacokinetics and narrow safety margin of PRX-MEA limits its therapeutic outcomes by conventional drug delivery systems. Due to lack of targeting ability using the intravenous and oral formulations available, PRX-MEA is not specifically distributed to the affected joints and rather gets accumulated in healthy tissues causing harmful side effects. In view of this, novel therapeutic strategies aiming to prevent joint destruction and associated comorbidities is highly desirable.[5] Transdermal drug delivery has the potential to reduce the side effects of PRX-MEA and to avoid first-pass elimination. Although the drug has been a subject of much research, a topical product of PRX-MEA is yet to be marketed.[6-8] At present, the permitted clinically useful transdermal application of PRX-MEA is with physical enhancement technologies such as iontophoresis, low-fluence erbium YAG laser or electroporation. Additionally novel carriers like deformable liposomes, novel temperature stimuli-responsive and biocompatible nanogels and solid in oil nanocarrier have been developed as promising nanocarriers for transdermal PRX-MEA delivery. A topical PRX-MEA formulation achieving optimal drug

concentrates in epidermis and effectively diminishing systemic toxicity would be of great utility for the treatment. Transdermal drug delivery would evade the GI-associated toxicities, first-pass metabolism related hepatotoxicity.[9-12]

Gold nanoparticles (AuNPs) can significantly improve drug delivery through the skin. Significant penetrations of small sized AuNPs through transdermal route have been reported earlier. AuNPs have numerous applications in biomedical sciences including drug delivery, tissue /organ imaging, photo thermal therapy and identification of pathogens in clinical specimens.[13-14] AuNPs are synthesized by the chemical reduction of chloroauric acid ($HAuCl_4$) using various reducing agents, the classical method pioneered by Turkevich et al for synthesis of monodispersed spherical 20 nm AuNPs using trisodium citrate.[15] AuNPs are easily tunable and different core sizes from 1 -150 nm can be synthesized by reduction process employing use of appropriate stabilizing agents to prevent particle agglomeration. Ease of synthesis, ready functionalization through thiol and amine linkages and modulation of drug release at remote place defines the versatility of AuNPs as drug delivery carrier. AuNPs have demonstrated enhanced pharmacokinetics, tumor tissue accumulations and the so called enhanced permeability and retention (EPR) effects *in vivo*. In its molecular form, gold compounds can serve as antiarthritic medications; hence AuNPs have been used for the treatment of Rheumatoid Arthritis for a very long time. Synovial angiogenesis plays a key role for the development of synovitis. Drug loaded AuNPs binds to vascular endothelial growth factor (VEGF) showing antiangiogenic effects on RA. Currently, biosynthesis of AuNPs has gained much attention and has emerged as an active research area in the field of nanotechnology.[16-18]

Oxidative damage and inflammation in various rheumatic diseases have been proved by increased levels of isoprostanes and prostaglandins in serum and synovial fluid compared to control.[19-20] Green tea polyphenols are effective inhibitory markers of oxidative stress that are secondary to an inflammatory response.[21-22] Green tea polyphenols also have been reported to act as both reducing and stabilizing agents for AuNPs synthesis by conjugating some of its components on the surface of AuNPs. Hence biosynthesis of AuNPs using green tea extract could offer therapeutic antioxidant effects both *in vitro* and *in vivo*.[23-25]

In the present study, we designed AuNPs as a carrier for the transdermal delivery of PRX-MEA. The reducing and stabilizing effects of green tea extract was exploited for the biosynthesis of AuNPs and subsequent loading of PRX-MEA. The key objectives were to improve the skin permeation of PRX-MEA and achieve better and sustained therapeutic efficacy by inhibition of pro-inflammatory biochemical markers which play a key role in synovial damage and progression of RA.[26-27]

MATERIAL AND METHODS

Materials

Commercial grade Piroxicam was a kind gift by Ramdev chemicals, Mumbai. Gold (III) Chloride trihydrate ($HAuCl_4.3H_2O$) was purchased from Himedia Laboratories, Mumbai. Tween 80 was obtained as a gift sample from Croda, India. Monoethanolamine, Diethanolamine, Triethanolamine were purchased from S.D. Fine chemicals Mumbai. 1, 1 diphenyl-2-picrylhydrazyl (DPPH) was obtained from Fluka labs sigma. Ascorbic acid was procured from Sisco Laboratories, Mumbai. All the other chemicals used were of Analytical grade.

Preparation of supersaturated drug solution.

Piroxicam has an aqueous solubility of 0.01 mg/mL at 20° C and is pH-dependent. To improve the solubility of Piroxicam, PRX-MEA salt with aqueous solubility of 1.472 mg/ml was prepared as described by Cheong & Choi.[6, 28] The supersaturated solutions of PRX-MEA were prepared at different concentrations of 1 mg/mL, 1.5mg/mL and 2mg/mL. The solution containing 1.5 mg/mL of PRX-MEA with was found to be stable and did not show recrystallization till 2 months and was used for further studies.

Selection of plant material and extraction

Commercially available TETLEY green tea bags were selected for the synthesis of AuNPs. The green tea stock solution was prepared by dipping one bag containing 1.85g of green tea leaves in 100ml methanol (HPLC grade) over a magnetic stirrer (1 MLH, Remi, India) for 30 min at room temperature. [29] The green colored tea extract was decanted gently and filtered through 0.45 µm Millipore membrane filter to remove the solid undissolved residues of tea leaves. The green filtrate was used as the reducing agent and was stored in the refrigerator at 8°C for further studies.

Preparation of PM-AuNPs

A calculated amount of PRX-MEA was added to the tea-initiated AuNPs, and followed by addition of 2.5 % V/V tween 80. The reaction mixture was stirred at 800 rpm for 120 min at room temperature and kept overnight in dark for complete reduction of gold ions and attachment of PRX-MEA to the nanogold surface. The PRX-MEA adsorbed AuNPs were recovered by centrifugation at 12,000 (Eltek RC 4100 D, Remi, Mumbai, India) for 30 min. The PRX-MEA adsorption on AuNPs surface was confirmed by UV-vis spectroscopy (Evolution 300 ™ UV-Vis Spectrophotometer. Thermo Scientific, USA). The UV spectrum was recorded in the range 300-600 nm. The formulation of PM-AuNPs was evaluated using a 3-factor 2-level factorial design with triplicate of center points with total 19. The data were analyzed and P-values less than 0.05 were considered to be statistically significant.[24]

Total phenolic content in the Green tea extract

The total phenolic content of the extract was estimated according to the method described by Ryan & Carolan.[30] The reaction mixture contained various concentrations of standard Gallic acid solution prepared in methanol, 1.5 ml of freshly prepared diluted Folin-Ciocalteu reagent (FCR) and 4 ml of 20% sodium carbonate solution. The final mixture was diluted to 15 ml with deionized water. Mixtures were kept in dark at ambient conditions for 2 h to complete the reaction. The absorbance was measured at 765 nm**.** The standard curve of absorbance verses concentration of Gallic acid was plotted. Similarly, aqueous and methanolic CS extract and PM-AuNPs were tested for the presence of phenolic catechins.

Total Phenolic content expressed as Gallic Acid Equivalents (mg of GAE/g dry weight of extract) were calculated using following equation;

$T = (C \times V) / M$

Where, T=Total content of phenolic compounds, milligram per gram dry weight of plant extract, in GAE; C= concentration of Gallic Acid established from the calibration curve, milligram per milliliter; V=the volume of extract, milliliter; M=the weight of methanolic plant.

Analysis of Particle size and zeta potential

Particle size of the AuNPs was determined by using Nanosight NS 500 (Malvern Instruments Ltd, UK) with computer controlled motorized stage and charge-couple device (CCD) that allows visualization and tracking of laser illuminated particles undergoing Brownian motion in suspension. 0.2 µl of the PM-AuNPs colloidal dispersion was diluted to 2 ml using ultrapure water and filtered using 0.22 µm nylon membrane filters to remove the contamination of dust and other particles. The samples were introduced directly into the chamber using a syringe. Video images were analyzed by NTA analytical software version 3.2. Measurements were carried out with red laser (638 nm) at 25 °C. Mean square displacement of particle, diffusion coefficient (Dt), sphere equivalent, hydrodynamic radius (rh) was determined using the Stokes- Einstein equation:

$$Dt = \frac{KBT}{6\pi\eta rh}$$

Where KB is Boltzmann's constant, T is the temperature and η is viscosity.

Zeta measurements were also performed using NTA. The zeta potential of AuNPs was measured on a particle-by-particle basis. The sample chamber is fixed with platinum electrodes, which allow a variable electric field to be applied to the nanoparticles suspended in aqueous solution. The measurement of the electrophoretic mobility for each tracked particle gives the zeta potential of the AuNPs.[26, 31]

Drug loading efficiency (% LE)

PRX-MEA loading onto AuNPs was expressed as the percentage of PRX-MEA in the produced nanoparticle with respect to the initial amount of PRX-MEA that was used for synthesizing the nanoparticles. [32] Drug loading efficiency (% LE) was analyzed by UV-Vis spectrophotometry (EVOLUTION 3000) in the dispersion after filtration through (mesh size 4 whatmann filter) to retain the unassociated PRX-MEA salt. The % LE was determined by the following equation:

$$LE\% = \frac{\text{Amount of drug added during preparation} - \text{amount of drug in the supernatant}}{\text{Amount of drug added during preparation}} \times 100$$

Lyophilization of AuNPs

The optimized AuNP pellets obtained after centrifugation were frozen at -20˚C overnight in deep freezer (Thermo scientific, India) followed by lyophilization at -80˚C at vacuum pressure 1 n Pa (labocon LBT-104, UK). The freeze dried AuNPs samples were further used for FTIR studies. [33]

UV-Vis sprectoscopy

The reduction of $HAuCl_4$ ions was monitored by measuring UV-Vis spectra in the range 300-600 nm. The overlay of UV-Vis spectra of blank and PRX-MEA loaded AuNPs were taken at room temperature on thermo scientific spectrophotometer using quartz cuvette and 1 cm optical path.[34]

***In –Vitro* release studies**

The *in-vitro* drug release of free PRX-MEA and PRX-MEA from AuNPs was investigated in Phosphate buffer (PB) pH 7.4. 2 mL of free PRX-MEA & 0.29 g/mL of PM-AuNPs aqueous solution was placed in dialysis bag (12000-14000 Da) and sealed tightly at both the ends with dialysis clips. The dialysis bag was immersed in 100 mL of release media, stirring at 37 ± 0.5°C at predetermined time points. 1 mL of sample was withdrawn and replenished with 1 mL of fresh release media. The studies were performed in triplicates. The release of PRX-MEA was analyzed by UV –Vis spectrophotometer at 354 nm. Data obtained from *in-vitro* release studies were fitted to various equations to investigate kinetics of drug release.[35]

***In- vitro* stability studies**

Stability studies of the optimized AuNPs were carried out at an ambient temperature of 28°C ± 3°C with 70% ± 10% relative humidity and at 8°C ± 2°C for 90 days. The samples were withdrawn at the predetermined time intervals of 0, 1, 30, 60, and 90 days and evaluated for appearance, particle size and % LE. To assess the storage stability, lyophilized optimized AuNPs was stored in a dessicator at 8°C ± 2°C and kept in a refrigerator for 60 days. Particle size measurements were made on day 0, after 30, and 60 days of strorage.[36]

Transmission electron microscopy (TEM)

The TEM images were acquired with Philips Tecnai-20 transmission electron microscope (Philips. Holland) with 0.27 nm point resolution and the accelerating voltage

was 200 kV. The copper grids coated with the concentrated optimized AuNPs dispersion and PM-AuNPs hydrogel were dried under IR lamp for 5-10 min. prior to the analysis.[32, 37]

FTIR measurements

FTIR spectra of free PRX, PRX-MEA and lyophilized optimized PM-AuNPs were recorded using Perkin Elmer- Spectrum RX-I FTIR, USA. FTIR specra were obtained over the scanning wavelength range 4,000-500 cm^{-1}.[24, 27,28]

XRD analysis

XRD analysis of the PRX-MEA powder, B-AuNPs and optimized PM-AuNPs drop coated onto glass substrates was carried out on a Phillips X' PERT PRO instrument equipped with a copper anode (Cu–Ka radiation, 45 kV, 40 mA k = 1.54405 nm) coupled to a detector. All measurements were recorded using a step width of 0.016°, a count time of 29.84 s, scanning range of 30.01° to 79.99° (2θ) scale and speed set between 20.02 to 80° per second. The results were analyzed using X'Pert Data Viewer version 1.2 software.[24,27,28]

Preparation of PM-AuNPs based hydrogel

The optimized PM–AuNPs were incorporated in carbopol based hydrogel matrix soaked overnight in water, suitable for transdermal application. Briefly, carbopol ulltrez 10 was dispersed into the solution of ultrapure water and glycerol (0.9:0.1% W/W) at concentrations of 1.5 % W/W. The resulting mixture was stirred for 3 h at room temperature using a magnetic stirrer (1 MLH, Remi, India) and neutralized with triethanolamine to yield a carbopol gel matrix with a pH value of 7. Optimized PM-AuNPs was mixed with an equal volume of the carbopol gel to form PM-AuNPs enriched hydrogel. The final concentration of carbopol was 0.75 % W/W. similarly, B-AuNPs enriched hydrogel was also prepared.[38]

Characterization of PM-AuNPs loaded hydrogel

PM-AuNPs enriched hydrogel was characterized for drug content, pH and spreadability.

Drug content

For determination of drug content, about 1g of gel was weighed in a 100 ml volumetric flask and dissolved in methanol. It was diluted appropriately with the mobile phase, methanol: water in the ratio of 60: 40 V/V and analyzed on a UV-spectrophotometer at 354 nm.

pH

The pH measurement of PM-AuNPs enriched hydrogel was done using a calibrated pen pH meter (Erma Inc.).

Spreadability

The spreadability was determined by placing 0.5 g of gel within a circle of 1 cm diameter pre–marked on a glass plate over which a second glass plate was placed. A weight of 500 g was allowed to rest on the upper glass plate for 5 min. The increase in the diameter due to spreading of the hydrogels was noted.

Rheological measurements

The rheological measurements of PM-AuNPs were performed on Brookfield CAP 2000 viscometer with spindle no. 0178-01 equipped with cone and plate geometry. All measurements were carried out at a temperature of 25°C ± 2°C. The position of the upward and downward curves in the rheogram was studied to determine the flow behavior. The effect of varying shear rate on the resulting shear stress was measured. The slope of the plot with log of shear stress versus log of shear rate represents the flow index and the antilog of the y-intercept represents consistency index. [38-39]

***In vitro* skin permeation study**

Pig ears were obtained post–sacrifice from a local abattoir (Raj pork shop, Charni Road Mumbai, India). The subcutaneous fat tissues were removed and hairs present were trimmed carefully without scratching the surface in ordered to ensure the barrier integrity. Excised skin was then carefully mounted on the diffusion cell with the SC side facing into the donor compartment while the dermal side faced downwards into the receptor compartment filled with modified Phosphate buffer pH 7.4. 2.2 ml of PRX-MEA solution (solubility: 1.472 mg/mL) and 0.5 g of optimized AuNPs enriched hydrogel were applied to the skin surface in the donor compartment which was covered to prevent evaporation. Air bubbles were eliminated from receptor phase via constant stirring throughout the experiment and the temperature was maintained at 37 ± 2 °C. After application of the test formulations, aliquots were collected at periodic time interval and analyzed for PRX-MEA content at the end of 24 h. All the skin permeation experiments were performed in triplicate. [40-42]

Interpretation of data

Cumulative amount of drug permeated at various time intervals was plotted as a function of time. The slope at the steady state concentration of the plot represents the flux (J_{ss}, µg/cm^2 /h). The permeability coefficient (K_p, cm/h) was calculated according to the following equation:

$$K_p = J_{ss}/C_d$$

Where, C_d is the concentration of the drug in the donor compartment.

The data expressed as mean ± SD and statistical analysis of the data was done using one way ANOVA followed by Dunnett's test. $P<0.05$ was considered as significant.

***Ex-vivo* skin corrosion studies**

Corrosive potential of PM-AuNPs gel was determined by Corrositex® test.[39] Corrosive substances destroy the epidermal proteins and cause color shift in the underlying chemical detection liquid. Corrosive potential was determined on porcine ear skin using 37 % nitric acid and 0.9 % W/V NaCl solutions as positive and

negative controls respectively. Skin samples were prepared and clamped on Franz diffusion cell. 200 µl of 37 % nitric acid solution, 0.9 % NaCl solution or PM-AuNPs gel was deposited onto the epidermis of the porcine skin. After 15 min, the sample was removed and the epidermis was further washed with 2 ml of distilled water to remove the residual sample. 1ml of Sulforhodamine B (skin proteins labeling dye) was deposited onto the epidermis. After 15 min, the dye was removed and the epidermis was washed. The experiment was conducted in triplicate. The absorbance of the washing water was measured with a spectrophotometer at 313 nm. The corrosive factor was calculated from the Eq. as shown below:

F= [Sample Absorbance-0.9 % NaCl solution Absorbance] / (0.9 % NaCl solution Absorbance).

Determination of *in vitro* antioxidant assay

The in vitro antioxidant and antiradical assays were conducted to evaluate the antioxidant status of PRX-MEA, B-AuNPs and PM-AuNPs.[43-47]

Sample preparation

The stock solutions of Piroxicam and ascorbic acid (positive control, PC) were prepared in methanol and B-AuNPs and PM-AuNPs were diluted in phosphate buffer pH 7.4 to obtain 1 mg/ml. Aliquots from the stock solutions were further diluted with the respective solvents as per the concentrations required. The concentrations used in all the assays were 50, 75, 100, 125 and 150µg/ml, respectively. The corresponding blank readings were also taken in all the assays. The percentage of free radical scavenging was calculated according to following equation.

$$\text{Scavenging/Inhibition\%} = A_{blank} - A_{sample} / A_{blank}$$

Where, A_{blank} is the absorbance of the blank and A_{sample} is the absorbance of the sample or PC.

DPPH free radical scavenging activity

The stable free radical-scavenging activity of PRX-MEA, B-AuNPs, PM-AuNPs and PC was determined by the DPPH assay as reported by Anandjiwala et al.[43] In its radical form, DPPH absorbs at 517 nm, but upon reduction by an antioxidant or a radical species, its absorption decreases. Lower absorbance of the reaction mixture indicates higher free radical scavenging activity. IC_{50} value is the concentration of the sample required to scavenge 50 % DPPH free radical.

Statistical analysis

All the experiments were carried out in triplicate and the results were expressed as mean ± SEM. The IC_{50} values were calculated using ED_{50} Plus v 1.0. Data were statistically analyzed by one-way ANOVA, followed by Student's t-test. $P<0.05$ was considered statistically significant.

Pharmacodynamics study (Protocol No.: KMKCP/IAEC/15106).

Model: Carrageenan Induced Paw Edema.[48-49]

Albino Wistar rats (150-200 g) were randomly divided into 5 groups of six animals each

Group I- Inflammatory Control: Carageenan solution (0.1ml of 1% W/V solution s.c.)

Group II- Placebo Gel: [Carbopol gel matrix + Carageenan (0.1 ml of 1% W/V solution)]

Group III- Standard drug: Conventional gel of piroxicam (marketed gel-Pirox®, 10mg/kg) + Carrageenan (0.1ml of 1% W/V solution s.c.)

Group IV- B-AuNPs enriched hydrogel + Carageenan (0.1ml of 1% W/V solution s.c.)

Group V- PM-AuNPs enriched hydrogel + Carageenan (0.1ml of 1% W/V solution s.c.)

The formulations will be applied transdermally to the right hind paw of albino rats of respective groups. After 30 min of transdermal application, 0.1 ml of 1% W/V carrageenan (in 0.9% normal saline) will be injected into the plantar region of the right hind paw of the rats to produce edema. The initial reading just after injection (at T=0) and subsequent paw volumes will be measured at the intervals of 1, 2, 3, 4, 6 and 24 h using a Digital Plethysmometer. The rate of edema formation and inhibition rate of each group will be calculated as follows:

Edema Rate (E %) = $V_t - V_o/V_o \times 100$

Inhibition Rate (I %) = $E_c - E_t/E_c \times 100$

Where, V_o is the mean paw volume before carrageenan injection, V_t the mean paw volume after the carrageenan injection at time t, E_c is the rate of edema formation of the toxicant group and E_t is the rate of edema formation of the treated group at time t.

Statistical analysis

The data were expressed as mean ± SEM and analyzed statistically using one way ANOVA followed by student's t-test using graphpad prism software v.5 (Graphpad software Inc. CA. USA) for comparison with arthritic control group. $P<0.05$ was considered as significant.

Stability studies

Storage stability of PM-AuNPs enriched hydrogel was conducted on day 0, 30, 60 and 90 days after storage at refrigeration conditions (8 °C ± 2°C). The homogeneity, phase separation, pH and drug content of the hydrogel were evaluated.[36]

RESULTS AND DISCUSSION

Total phenolic content

We determined the total phenolic catechins present in the Camellia sinesis (CS) extract by the Folin-Ciocalteu method. Quantitative determination of total phenols in CS extract was done on the basis of a standard curve of gallic acid ($y=0.0029x+0.0498$. $R^2= 0.999$). The percentage of total phenols in the methanolic CS extract was found to be 39.3 ± 0.25 % W/W whereas, for aqueous CS extract this value is lower and found to be 16.87 ± 0.52% W/W as shown in Fig. 1.[30] Additionally, PM–AuNPs were tested for the presence of phenolic

catechins. The value of 9.43 ± 0.19 % W/W, indicated that during initiation of the reduction process catechins also gets attached to the surface of AuNPs based on their affinity towards nanogold.

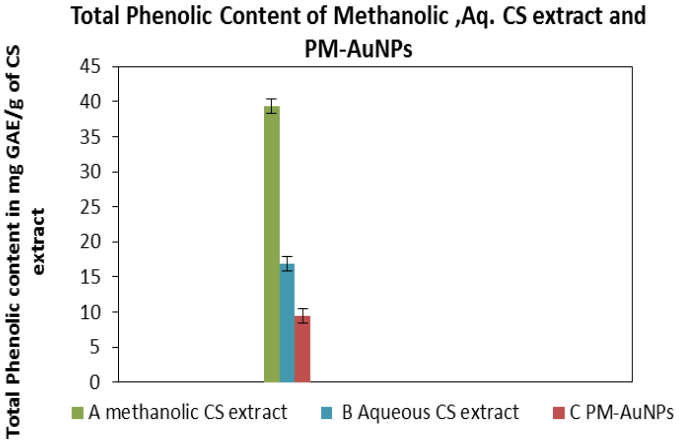

Fig.1 Total polyphenolic content of A) Methanolic CS extract B) Aqueous CS extract C) PM-AuNPs.

Preparation of B-AuNPs and PM-AuNPs

Tea phytochemicals have been reported to serve a dual role as effective reducing agents as well as stabilizers. However our preliminary studies with green tea extract alone as a reducing agent and stabilizer resulted in B-AuNPs with higher polydispersity index and exhibited particle agglomeration within a week after preparation. The particles size of B-AuNPs was found to be 106.7 ± 78.7nm.

In order to achieve B-AuNPs with a robust coating of protective agent, tween 80 a polymeric non-ionic surfactant was chosen as stabilizer.[50-51] The enhanced stability of AuNPs in the presence of tween 80 can also be explained through static electricity repulsive forces, steric hindrance and Van der Waals forces exerted by the surfactant molecules through adsorption on to AuNPs surface. The particle size of B-AuNPs was found to be 33.5 ± 90.3nm. The zeta potential of B-AuNPs displayed the zeta value -21.8 ± 15.6 mV, indicating a negative charge on the surface of nano particles. Synthesis of PM-AuNPs in combination of tea polyphenols as reducing agents and tween 80 as stabilizer represents an easy inexpensive, green and user-friendly biosynthetic process.

Synthesized B-AuNPs were confirmed by UV visible spectroscopy the colour change from pale yellow to ruby red after the completion of the reaction confirms the formation of B-AuNPs in the nano dimension. PRX-MEA binding to the surface of B-AuNPs resulted in formation of PM-AuNPs.

UV-spectroscopy

The UV-Vis absorption spectra of B-AuNPs solution recorded after 24 h of reaction showed the peak of maxima at 538 nm attributed to the surface Plasmon resonance (SPR) band of B-AuNPs. Synthesized PM-AuNPs were confirmed by UV-Vis spectroscopy. The UV spectra of PM-AuNPs displayed a gold SPR band centered at 554 nm shown in Fig. 2. Additionally, the peak observed at 354 nm could be attributed to PRX-MEA.

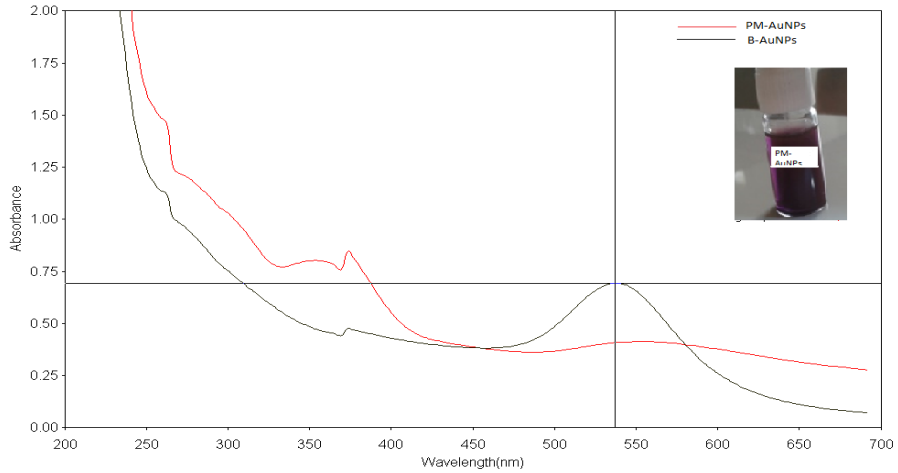

Fig. 2 UV spectra of blank AuNPs and PRX-MEA loaded AuNPs.

The shifting of SPR band from B-AuNPs to PM-AuNPs was observed as binding of PRX-MEA to the AuNPs surface can change the Plasmon resonance frequency directly. Further as the particle size increases the wavelength of SPR related absorption shifts to the larger wavelength. This was also reflected in the change of color of PM-AuNPs from ruby red to dark purple.

Zeta potential and Particle size

The zeta potential and particles size distribution of the optimized formulations is shown in Fig. 3 and Fig. 4 respectively. The mean particle size and calculated zeta potential of PRX-MEA –AuNPs was 51.2 ± 33.8 nm and -30.2 ± 14.2 mV. The observed reduction of zeta potential could be attributed due to the binding of PRX-MEA on to the surface of AuNPs. Similar observations have been reported by Honary et al.

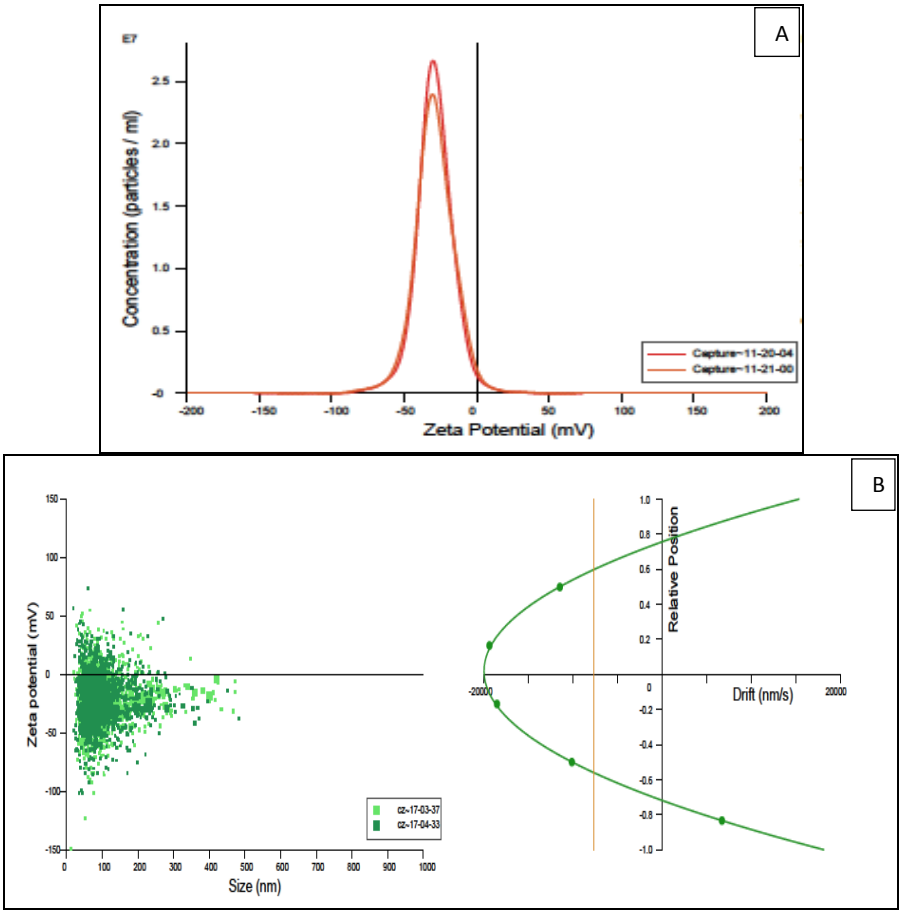

Fig. 3 Zeta potential of optimized formulations PM-AuNPs A) zeta potential versus concentration curve B) particle size versus zeta potential intensity plot

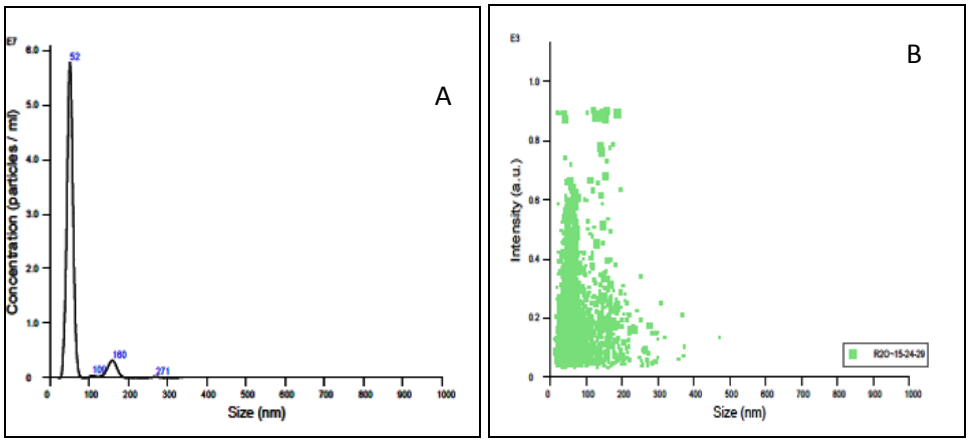

Fig. 4 Particle size distribution of the optimized formulation PM-AuNPs, A) particle size versus concentration profile of PM-AuNPs B) particle size versus intensity of PM-AuNPs

The lyophilized PM-AuNPs powder was dark purple in colour and easily reconstituted in HPLC water. Also no aggregation after reconstitution was observed. Lyophilized B-AuNPs were easily dispersible too. The particle size of lyophilized PM-AuNPs was 58.7 ± 156.7 nm. The reproducibility of the method for synthesis of PM-AuNPs was studied by fabricating a batch of PM-AuNPs-C and the particle size was found to be 59.7 ± 88.8 nm. No significant diffrerence between the particle size of PM-AuNPs and its PM-AuNPs-C batch was found. The above result indicates batch to batch reproducibility of the method for AuNPs preparation.[51]

***In vitro* release studies**

Fig. 5 shows the cumulative drug release of free PRX-MEA and PM-AuNPs. The percentage cumulative drug release at the end of 48 h for PM-AuNPs was found to be 91.24 ± 3.48 %. The free PRX-MEA showed more than 80% release in 6h. The percentage cumulative release at the end of 6 h for free PRX-MEA was found to be 90.14 ± 3.54 % Contrary to this, PM-AuNPs exhibited a biphasic release at the end of 4 h, the cumulative PRX-MEA release from AuNPs was found to be 6.20 ± 0.65% followed by sustained released till 48 h. The burst release observed may be due to loosely attached PRX-MEA molecules present on the AuNPs surface. The methods of approach to investigate the kinetic of drug release of the formulations were zero-order, first-order, Higuchi model, korsmeyer-peppas and Hixon-Crowell model.

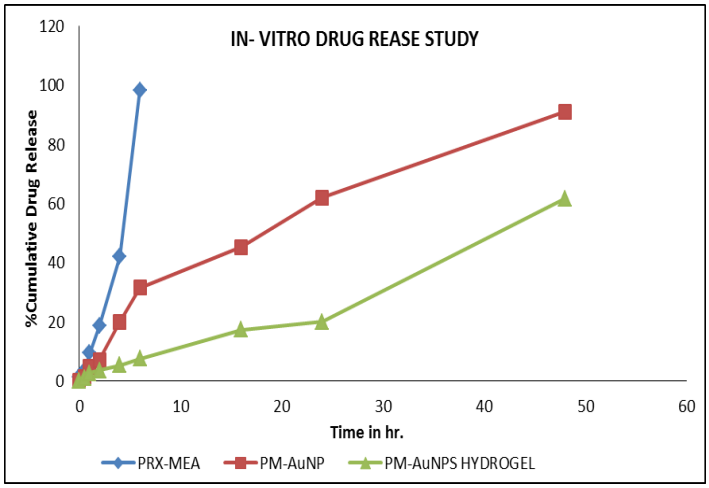

Fig. 5 Release profile of free PRX-MEA from PM-AuNPs and at 37 ± 0.5°C each point represents mean ± SD (n=3).

The mechanism of drug release from PM-AuNPs is diffusion controlled and follows Higuchi model (R^2=0.968). The Higuchi model is a concentration dependent process based on Fickian diffusion. The release of PRX-MEA is dependent on the diffusion of water into the naroparticles followed by detachment of PRX-MEA and finally diffusion of dissolved PRX-MEA from AuNPs.

***In vitro* stability studies**

There was a little increase in the particle size of PM-AuNPs stored at 28°C ± 3°C for a period of 90 days. The particle size and the standard deviation from day 0 to day 30 were increased from (51.2 ± 46 nm to 62.5 ± 88 nm) However , there was no drastic increase in the particle size. The sedimentation of AuNPs was observed post 60 days; however the sediment was easily dispersible upon shaking. Similar observations were recorded at 8°C ± 2°C as shown in the Table no. 1.The particle size increased from 51.2 ± 38.5 nm to 61.7 ± 81nm after 90 days of storage. The % LE of PM-AuNPs was found to be 89.05± 0.41% on day 0 and 76.16. ± 0.51% after 30 and 60 days of storage at 28°C ± 3°C respectively. Similarly, the % LE of PM-AuNPs was found to be 89.52 ± 0.55 % and 77.55 ± 0.53 % after 90 days of storage at 8°C ± 2°C respectively. Hence the particle size and % loading efficiency of PM-AuNPs did not change drastically even after the end of three months.

Table no. 1 Stability of the optimized formulation (PM-AuNPs) after storage at 0, 1, 30, 60 and 90 days at (A) 28°C ± 3°C; (B) 8°C ± 2°C.

Period of observation (days)	PS		EE	
	8°C ± 2°C	28 °C ± 3°C	8°C ± 2°C	28 °C ± 3°C
0	51.2 ± 38.5nm	51.2 ± 46nm	89.52 ± 0.55%	89.05 ± 0.41%
30	54.3 ± 57nm	52.8 ± 59nm	86.67 ± 0.67%	86.32 ± 0.63%
60	55.4 ± 76nm	56 ± 67nm	82.4 ± 0.68%	83.79 ± 0.47%
90	61.7 ± 81nm	62.5 ± 88nm	77.55 ± 0.53%	76.16 ± 0.51%

Data Expressed as Mean ± SD, n=3

Transmission Electron Microscopy (TEM) observations

TEM has been extensively used to investigate the morphology, size and selected area electron diffraction (SAED) of AuNPs. As shown in Fig. 6(A), the typical TEM image of PM-AuNPs Synthesized by reduction of $HAuCl_4$ exhibit mostly spherical shape nanoparticles, however few nanoparticles were triangular, pentagonal and rod shaped. The corresponding SAED pattern of the biosynthesized AuNPs is shown in Fig. 6(B). Each ring corresponds to diffraction pattern of the crystalline gold structure. Multiple rings in SAED pattern indicates polycrystalline nature of PM-AuNPs which is in agreement with XRD patterns. As shown in Fig. 6(C), the TEM photomicrographs confirmed the presence of AuNPs in hydrogel were also in spherical shape.

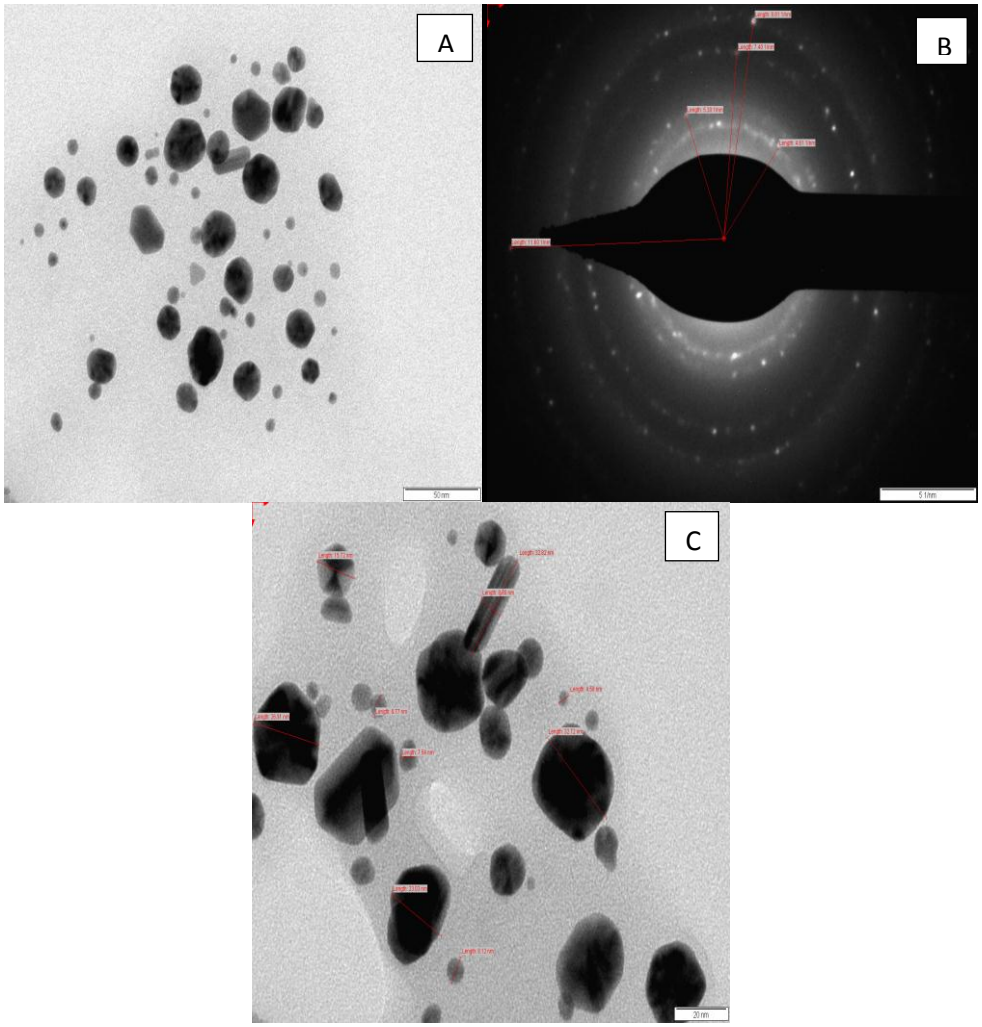

Fig. 6 TEM image of A) PRX-MEA loaded gold nanoparticle and B) the SAED pattern. C) PM-AuNPs enriched gel. The scale Bar corresponds to nm.

FTIR measurements

The FTIR spectrum of PRX contains a sharp peak at 3337.96 cm^{-1} attributed to NH and OH group as stated in literature.[27] The absence of this peak in PRX-MEA indicated the strong intermolecular interaction between Piroxicam and the ethanolamine. Peaks in the range of 1500-1680 can be attributed to C-N or NH_2 vibrations. In the FTIR spectrum of PM-AuNPs the N-H stretching peak of PRX-MEA shifts towards a higher wave number (3733.58 cm^{-1}) and thus indicates possible binding of the $–NH_2$ group of free PRX-MEA with gold surface via Au:N interactions as shown in Fig.7. The characteristic carboxylic acid peak in the free PRX-MEA spectrum at 2952.26 cm^{-1} shifted to higher wavelength region and was immersed into the $–NH_2$ peak (3399.5 cm^{-1}) when PRX-MEA conjugated to AuNPs suggesting and interaction between NH_2 and gold. Similar observation has been reported by Tran et al. Furthermore, the broad peak observed at 1513.22cm^{-1} corresponds to C=C vibrations of aromatic structures and C=O stretching of amide and carboxylic acids as observed in the FTIR spectra of dried green tea powder. The peak observed at 765 cm^{-1} was attributed to primary and secondary amines and amides. The PM-AuNPs spectra exhibited characteristic peaks of both polyphenol molecules and PRX-MEA.

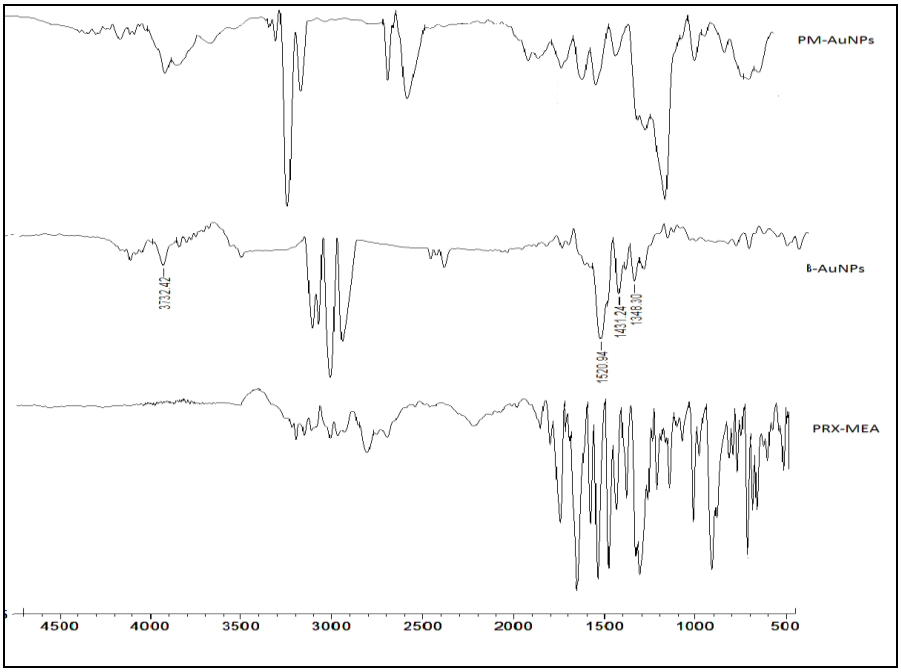

Fig. 7 FTIR spectra of A) PRX-MEA B) lyophilized B-AuNPs. C) Lyophilized PM-AuNPs

XRD analysis

The diffraction pattern of PRX-MEA exhibited distinct sharp peaks at 20.53°, 21.65°, 22.95°, 25.96°, 27.67°, 28.03°, 31.28°. The crystalline structure of gold nanoparticles was confirmed by XRD analysis. The Fig. 8 shows XRD pattern of PM-AuNPs and B-AuNPs deposited on the glass substrates. XRD analysis revealed the intense peaks of reflected radition (Bragg peaks) at 38.13° (111), 44.33° (200), 64.58° (220) and 77.69° (311) planes respectively and were indexed to the diffraction lines of the face-centered cubic (fcc) gold with very small crystallite energy. The predominant orientation was the (111) plane because the most intense peak appeared at 38.13°. The diffraction peaks observed are well in agreement with the International Centre for Diffraction Data 10725392 of bulk gold, which further corroborates the formation of crystalline gold. Similar observations have been reported by Tran et al and his collaborators. They reported characteristic crystal planes of the fcc crystal structure of gold nanoparticle synthesized using methotrexate as both the reducing agent and the capping molecule. The diffraction pattern of PRX-MEA showed remarkable difference from those of PM-AuNPs and B-AuNPs. From Fig. 8 it can be observed that the sharp diffraction peaks of PRX-MEA could not be detected in diffractogram of PM-AuNPs which indicates that PRX-MEA was loaded onto the surface of AuNPs and stabilized in amorphous form. This suggests that the drug was successfully loaded on to the surface of gold. Also, as there was not much difference (except some extra peaks at 21.06°, 26.43°, 29.03°, 32.52° due to the binding of PRX-MEA) in the diffraction pattern of the B-AuNPs and PM-AuNPs, it is justified that addition of PRX-MEA did not change the crystalline nature of the gold nanoparticles.

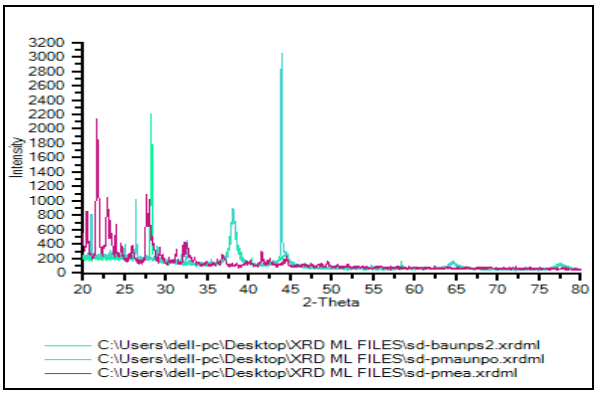

Fig. 8 XRD pattern of synthesized PM-AuNPs.

Preparation of PM-AuNPs based hydrogel

PM-AuNPs enriched hydrogel was successfully fabricated as shown in Fig. 9. The developed formulation was light purple in color with no odor, homogenous, smooth in feel and did not show any phase separation. The hydrogel was free from grittiness, which reflects the

degree of acceptability of formulation by patients. The pH of the hydrogel was found to be 6.82 ± 0.02, reflecting no risk of skin irritation. The PRX-MEA content of the PM-AuNPs hydrogel was found to be 95.34 ± 2.39 % of the theoretical value. The spreadability of PM-AuNPs hydrogel was found to be 5.79 ± 0.54 cm. The incorporation of PM-AuNPs did not affect the spreadability of plain gel base with almost similar spreadability values indicating easy spreading on the skin.

Fig. 9 Blank gold nanoparticles and PRX-MEA loaded gold nanoparticles enriched hydrogel

Rheological measurements

PM-AuNPs colloidal dispersion was converted to a suitable semisolid dosage form because of its low viscosity and inability to retain on the skin for transdermal delivery. PM-AuNPs loaded hydrogel was characterized for its rheological properties and comparison was made with plain carbopol gel base. The analysis plot (power law) of the carbopol gel matrix and PM-AuNPs hydrogel and Marketed Pirox gel are shown in Fig. 10. According to the power law analysis plot, the consistency index and flow index for carbopol gel were 1382 and 0.13 respectively. The consistency index and flow index for PM-AuNPs hydrogel were 848 and 0.35 respectively whereas, for Marketed Pirox gel these values were 611.7 and 0.38 respectively. The viscosity of carbopol gel, PM-AuNPs hydrogel and Pirox gel at 50 rpm was found to be 14.10 ± 0.01, 11.95 ± 0.12 and 10.91 ± 0.29 poise respectively. The higher values of consistency index, flow index and viscosity signified that the PM-AuNPs hydrogel is better than the marketed formulation in terms of rheology. The incorporation of PM-AuNPs in gel matrix resulted in flow index of 0.35, indicating pseudoplastic flow. This pseudo plasticity results from the network that aligns itself in the direction of shear, thereby decreasing the viscosity as the shear rate increases. The plastic viscosity η (Bingham plot) was found to be 2.91 and 2.78 for carbopol gel and PM-AuNPs hydrogel respectively. The flow behavior exhibited by the gels indicated its suitability for transdermal application.

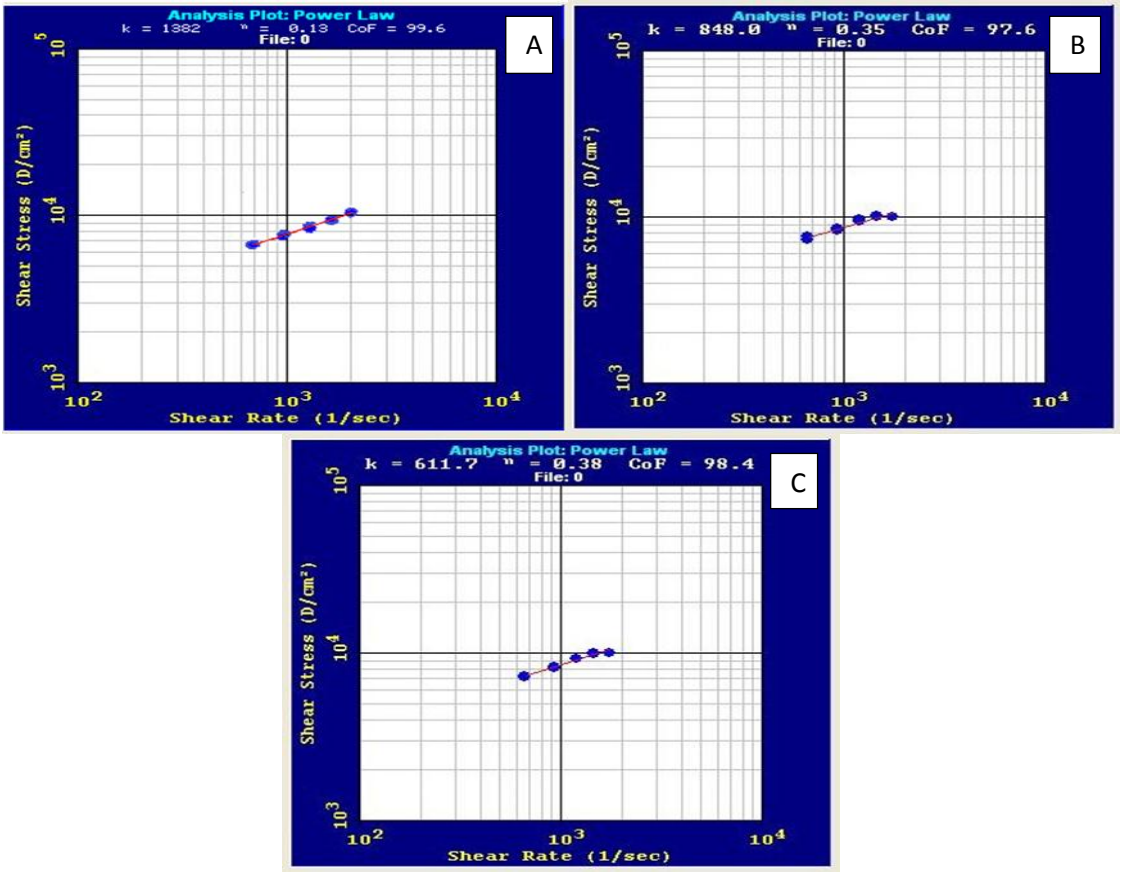

Fig. 10 Power law analysis plot of A) Carbopol gel matrix and B) PM-AuNPs hydrogel C) Marketed Pirox^{R} gel showing correlation between shear rate and shear stress.

In vitro skin permeation study

The percutaneous parameters of tested formulation are given in Table no. 2. Cumulative amount of PRX-MEA permeation after 24 h is as shown in Fig. 11. The cumulative amount of PRX-MEA permeated from PM-AuNPs and PM-AuNPs enriched hydrogel were significantly higher than plain PRX-MEA solution ($P<0.01$). Incorporation of PM-AuNPs into hydrogel delayed PRX-MEA release as AuNPs are entrapped into a three dimensional network of carbopol hydrogel and the release rate of the drug from this gel matrix governs the skin penetration.

Table no. 2 Permeation kinetic parameters of the tested formulation means ± SD; n=3

Formulation code	Percutaneous permeation parameters	
	J_{ss}(µg/cm^2/ h)	Kp(Cm/h)×10^{-4}
PRX-MEA solution	2.69 ± 0.19	8.56 ± 0.52
PM-AuNPs	8.23 ± 0.07**	28.51 ± 0.36**
PM-AuNPs hydrogel	4.91 ± 0.32**	14.70 ± 2.09**

,$J_{ss:}$ steady state reflux Kp: permeability coefficient, Data expressed as means ± SD; n=3
*** P<0.01: statistically significant as compared to plain PRX-MEA solution.*

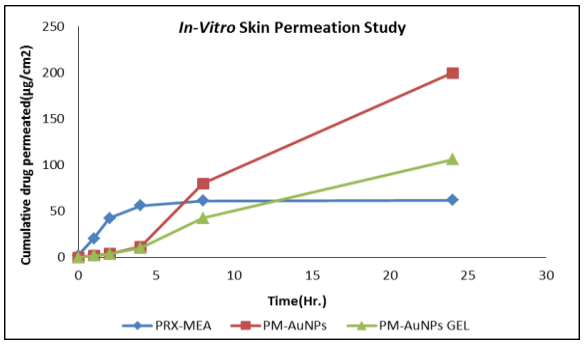

Fig. 11 comparative skin permeation profiles of PM-AuNPs and PM-AuNPs hydrogel with PRX-MEA solution

Transdermal delivery of PRX-MEA (hydrophilic molecule) is challenging. The water solubility and charged structure of PRX-MEA limits its skin permeation through the highly organized microstructure of stratum corneum. However AuNPs have a high potential to interact with the skin barrier, leading to increase in skin permeability and enhancement of payload delivery to deeper skin layers .Thus, AuNPs as transdermal carrier is suitable to enhance the skin permeation of PRX-MEA. The nano-sized AuNPs facilitates their contact with skin corneocytes and support drug permeation into viable skin; additionally the negative charged particles have been reported to augment permeation through skin.

***Ex-Vivo* Skin Corrosion Study**

The experiment was conducted in triplicate. The results are shown in Table no. 3.
If F>0, then the sample is non-corrosive.
If F<0, then the sample is corrosive.
As observed, PM-AuNPs dispersion fits in F>0 criteria hence found to be non-corrosive as compared to the positive control.

Table no. 3 Corrosive factor of the formulations

Formulation	Corrosive Factor (F)
37% Nitric acid solution (positive control)	-0.75341± 0.72
PM-AuNP loaded hydrogel	0.925 ± 0.018

Data is expressed as Mean ± SD (n=3).

DPPH free radical scavenging activity

The formulations showed free radical scavenging potential in the *in vitro* model described in Table no. 4. PM-AuNPs showed almost similar, although statistically insignificant antioxidant activity as compared to PC in the DPPH. It was observed that free radicals were scavenged by PM-AuNPs in a concentration dependent manner. On a comparative basis, PM-AuNPs showed superior antioxidant activity than pure drug.

Table no. 4 Effect of formulations on free radical scavenging activity.

Model studied	IC_{50} (g/ml)			
	PRX-MEA	B-AuNPs	PM-AuNPs	PC
DPPH activity	96.78± 0.53***	66.38 ± 0.25	44.76 ± 06	50.74 ±1.62

*PC: positive control (Ascorbic acid), data is expressed as mean ± SEM; n=3; *** P<0.001 significantly different as compared to PC.*

Pharmacodynamic studies (Protocol No.: KMKCP/IAEC/15106).

In the present study, In order to evaluate the therapeutic effect of PM-AuNPs enriched hydrogel, Carageenan was used to initiate edema in rats attributed to two phases; release of histamine and serotonin followed by release of prostaglandins and lysosomal bodies which are sensitive to most clinically effective anti-inflammatory drugs.

After single injection of carrageenan a rapid reliable, robust and easily measurable edema was developed. This model closely resembles to the arthritic swelling seen in human RA. Application of PM-AuNPs enriched gel and the standard marketed gel resulted in 97.75 ± 4.02% and 67.17 ± 2.55% inhibition of edema after 24hrs as shown in Figure 12. There is a significant difference between the tested groups and the arthritic control as determined by a one way ANOVA with $P < 0.001$.[49]

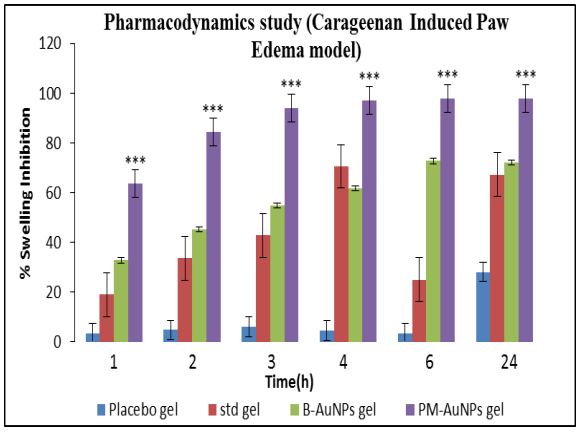

Fig. 12 Effects of PM-AuNPs hyrogel on edema of the rats. Data is expressed as mean ± SEM; (n=6). ***P<0.001 vs. the arthritic control group.

Stability studies

The physical characteristics, pH and drug content of PM-AuNPs enriched hydrogel at different storage time intervals are shown in Table no. 5. The PM-AuNPs hydrogel was stable with no significant change in homogeneity and pH throughout the storage period. There was no notable change in the drug content of the formulation after 90 days storage at refrigeration temperature. These observations indicate good physical stability of the PM-AuNPs hydrogel.

Table no. 5 The physical characteristics, pH and drug content of PM-AuNPs enriched hydrogel at different storage time intervals.[51]

Sr.No.	parameters	Observations			
		0^{th} day	30^{th} day	60^{th} day	90^{th} day
1	Color	Light purple	Light purple	Light purple	Light purple
2	Homogeneity	Yes	Yes	Yes	Yes
3	pH	6.82 ± 0.02	6.82 ± 0.02	6.85 ± 0.02	6.86 ± 0.03
4	Drug content %	95.34 ± 2.39	94.47 ± 1.54	92.90 ± 1.21	90.22 ± 1.50

pH and % Drug content were erxpressed as Mean ± SD^2, n=3

CONCLUSION

The most significant finding of this study was that PM-AuNPs were successfully fabricated using bioreduction by green tea extract with minimum particle size, high PRX-MEA loading and excellent storage stability at different temperature. PM-AuNPs were developed using 2^3 full factorial design approaches and evaluated by UV spectroscopy, TEM, XRD, FTIR. PM-AuNPs displayed characteristic surface plasmon resonance. It was also exhibited that PRX-MEA loaded AuNPs were capable of releasing PRX-MEA in a slow and sustained manner. Furthermore PM-AuNPs enriched hydrogel for transdermal delivery was developed and evaluated. The *in vitro* skin permeation kinetics indicated that both PM-AuNPs dispersion and hydrogel enhanced the steady state flux and permeation coefficient of PRX-MEA. The *Ex –vivo* corrosive study showed that the formulation was not corrosive to the skin. In the Free radical scavenging assay PM-AuNPs possesses remarkable activity as compared to the free PRX-MEA. Therefore, PM-AuNPs formulation could serve as a better alternative for treating rheumatoid arthritis by improving the therapeutic activity.

ACKNOWLEDGEMENTS

We would also like to acknowledge TIFR for conducting the PXRD study and Tem lab IIT Bombay for TEM study. We would like to acknowledge Ramdev chemicals for the generous gift sample of Piroxicam.

REFERENCES

1. Firestein GS. Etiology and pathogenesis of rheumatoid arthritis. In: Edward D, Genovese MC, Firestein GS, Sargent JS, Sledge CB (eds) Kelley's textbook of rheumatology, 9th edn, Philadelphia; Elsevier Saunders, 2005; 996–1042.
2. Mahajn A, Tandon VR, Antioxidants and rheumatoid arthritis. J Indian Rheumatol Assoc, 2004; 12: 139-142.
3. Dannhardt G, Kiefer W. Cyclooxygenase inhibitors – current status and future prospects. European

Journal of Medicinal Chemistry, 2001; 36(2): 109-126.
4. Marnett L, DuBois R. COX-2: A Target for Colon Cancer Prevention. Annual Review of Pharmacology and Toxicology, 2002; 42(1): 55-80.
5. Quan L, Thiele G, Tian J, Wang D. The development of novel therapies for rheumatoid arthritis. Expert Opinion on Therapeutic Patents, 2008; 18(7): 723-738.
6. Gwak H, Choi J, Choi H. Enhanced bioavailability of piroxicam via salt formation with ethanolamines. International Journal of Pharmaceutics, 2005; 297:156–161.
7. Gow P. A multi-centre study of piroxicam in the treatment of osteoarthritis and rheumatoid arthritis in general practice. Current Medical Research and Opinion, 1983; 8(9): 618-621.
8. Biemond P, Han H, Swaak A, Koster J. Diminished Superoxide Production of Synovial Fluid Neutrophils in Patients with Rheumatoid Arthritis Following Piroxicam Treatment. Scandinavian Journal of Rheumatology, 1990; 19(2): 151-156.
9. Lamoudi L, Chaumeil J, Daoud K. PLGA Nanoparticles Loaded with the Non-Steroid Anti-Inflammatory: Factor Influence Study and Optimization Using Factorial Design. International Journal of Chemical Engineering and Applications, 2013; 369-372
10. Ostwald W. An Introduction to Theoretical and Applied Colloid Chemistry. New York; John Wiley and Sons, 1917; 23.
11. Kreutzer, J. Colloidal drug delivery system, Drug and Pharmaceutical Sciences. New York; Marcel Dekker, INC, 1994; 20-48.
12. Ah Y, Choi J, Choi Y, Ki H, Bae J. A novel transdermal patch incorporating meloxicam: In vitro and in vivo characterization. International Journal of Pharmaceutics, 2010; 385(1-2): 12-19.
13. Dreaden EC, Alkilany AM, Huang X, Murphy CJ, EI Sayed MA. The golden age; gold nanoparticles for biomedicine. Chem Soc Res.**,** 2012; 41: 2740-2779.
14. Lee H, Lee M, Bhang S et al. Hyaluronate–Gold Nanoparticle/Tocilizumab Complex for the Treatment of Rheumatoid Arthritis. ACS Nano, 2014; 8(5): 4790-4798.
15. Kimling J, Maier M, Okenve B, Kotaidis V, Ballot H, Plech A. Turkevich Method for Gold Nanoparticle Synthesis Revisited. The Journal of Physical Chemistry B, 2006; 110(32): 15700-15707.
16. Uppal M, Kafizas A, Ewing M, Parkin I. The room temperature formation of gold nanoparticles from the reaction of cyclohexanone and auric acid; a transition from dendritic particles to compact shapes and nanoplates. Journal of Materials Chemistry A, 2013; 1(25): 7351.
17. Zabetakis K, Ghann W, Kumar S, Daniel M. Effect of high gold salt concentrations on the size and polydispersity of gold nanoparticles prepared by an extended Turkevich–Frens method. Gold Bulletin, 2012; 45(4): 203-211.
18. Ahmad T, Khan W. Size Variation of Gold Nanoparticles Synthesized Using Tannic Acid in Response to Higher Chloroauric Acid Concentrations. World Journal of Nano Science and Engineering, 2013; 03(03): 62-68.
19. Desai PB, Manjunath S, Kadi S,Chetana K, Vanishree J. Oxidative stress and enzymatic antioxidant status in rheumatoid arthritis: a case control study. Eur Rev Med Pharmacol Sci., 2010; 14: 959–967.
20. Gelderman K, Hultqvist M, Olsson L et al. Rheumatoid Arthritis: The Role of Reactive Oxygen Species in Disease Development and Therapeutic Strategies. Antioxidants & Redox Signaling, 2007; 9(10): 1541-1568.
21. Ahmed S. Green tea polyphenol epigallocatechin 3-gallate in arthritis: progress and promise. Arthritis Research & Therapy, 2010; 12(2): 208.
22. Marino A, Paterniti I, Cordaro M et al. Role of natural antioxidants and potential use of bergamot in treating rheumatoid arthritis. PharmaNutrition, 2015; 3(2): 53-59.
23. Sharma R, Gulati S, Mehta S. Preparation of Gold Nanoparticles Using Tea: A Green Chemistry Experiment. Journal of Chemical Education, 2012; 89(10): 1316-1318.
24. Konwar Boruah S, Kumar Boruah P, Sarma P, Medhi C, Kumar Medhi O. Green Synthesis Of Gold Nanoparticles Using Camellia Sinensis And Kinetics Of The Reaction. Advanced Materials Letters, 2012; 3(6): 481-486.
25. Forester SC, Lambert JD. Antioxidant effects of green tea. Mol. Nutr. Food Res, 2011; *55*: 844-854.
26. Shaji J, Varkey D. Silica-Coated Solid Lipid Nanoparticles Enhance Antioxidant and Antiradical Effects of Meloxicam. J Pharm Investig, 2013; 43(5): 405–416.
27. Rodrigues M, Calpena A, Amabilino D, Ramos-López D, de Lapuente J, Pérez-García L. Water-soluble gold nanoparticles based on imidazolium gemini amphiphiles incorporating piroxicam. RSC Advances, 2014; 4(18): 9279.
28. Cheong HA, Choi HK. Enhanced percutaneous absorption of piroxicam via salt formation with ethanolamines. Pharm Res, 2002; 19: 1372–1377.
29. Perva-Uzunalić A, Škerget M, Knez Ž, Weinreich B, Otto F, Grüner S. Extraction of active ingredients from green tea (Camellia sinensis): Extraction efficiency of major catechins and caffeine. Food Chemistry, 2006; 96(4): 597-605.
30. Ryan L, Carolan S. Determination of the total antioxidant capacity and total polyphenol content of commercially available green tea. Proceedings of the Nutrition Society, 2011; 70(OCE4).
31. Honary S, Zahir F. Effect of Zeta Potential on the Properties of Nano-Drug Delivery Systems - A Review (Part 1). Tropical Journal of Pharmaceutical Research, 2013; 12(2).

32. Verma VK., Ram K. Preparation, characterization and in-vitro release of piroxicam loaded Solid lipid Nanoparticles. International journal of pharmaceutical sciences and nanotechnology, 2014; *7*: 2338-2345.
33. Youngren S, Mulik R, Jun B, Hoffmann P, Morris K, Chougule M. Freeze-Dried Targeted Mannosylated Selenium-Loaded Nanoliposomes: Development and Evaluation. AAPS Pharm SciTech, 2013; 14(3): 1012-1024.
34. Link SEl-Sayed M. Size and Temperature Dependence of the Plasmon Absorption of Colloidal Gold Nanoparticles. The Journal of Physical Chemistry B, 1999; 103(21): 4212-4217.
35. Rasool B, Azeez O, Lootah H, Abusharbain I, Abu-Alhaj H, Nessa F. Extended Release Niosomal Hydrogel for Ocular Targeting of Piroxicam: In vitro and Ex vivo Evaluation. British Journal of Pharmaceutical Research, 2014; 4(21): 2494-2510.
36. ICH. Q1A (R2) - Stability Testing of New Drug Substances and Products. History, 2003; February, 24.
37. Kiran Babu S. Formulation and In-Vitro Evaluation of Piroxicam Loaded BSA Nanospheres by Desolvation. Journal of Nanomedicine & Nanotechnology, 2015; 06(03).
38. Zhao Y, Wang Z, Zhang W, Jiang X. Adsorbed Tween 80 is unique in its ability to improve the stability of gold nanoparticles in solutions of biomolecules. Nanoscale, 2010; 2(10): 2114.
39. Verma VK., Alpana R. Development of Piroxicam loaded SLN- based hydrogel for Transdermal Delivery. International journal of pharmaceutical sciences and nanotechnology, 2010; 3: 1136-1146.
40. Sujitha B, Krishnamoorthy B, Muthukumaran M. Formulation and Evaluation of Piroxicam Loaded Ethosomal Gel for Transdermal Delivery. Int J Adv Pharm Gen Res., 2014; *2:* 34-45.
41. Jain S, Jain P, Umamaheshwari R, Jain N. Transfersomes—A Novel Vesicular Carrier for Enhanced Transdermal Delivery: Development, Characterization, and Performance Evaluation. Drug Development and Industrial Pharmacy, 2003; 29(9): 1013-1026.
42. Nayak AK, Mohanty B, Sen KK. Comparative Evaluation of *Invitro* Diclofenac sodium Permeability across Excised Mouse Skin from Different Common Pharmaceutical Vehicles. Int. J. Pharm Tech Res, 2010; 2(1): 920–930.
43. Cheong H, Choi H. Effect of ethanolamine salts and enhancers on the percutaneous absorption of piroxicam from a pressure sensitive adhesive matrix. European Journal of Pharmaceutical Sciences, 2003; 18(2): 149-153.
44. Anandjiwala SH, Srinivasa K, Rajani M Free radical scavenging activity of Bergia suffruticosa (Delile) Fenzl. J Nat Med, 2007; 61: 59–62.
45. Ghorbani H. Green Synthesis of Gold Nanoparticles. Oriental Journal of Chemistry, 2015; 31(1): 303-305.
46. Yashin A, Yashin Y, Nemzer B. Determination of Antioxidant Activity in Tea Extracts, and Their Total Antioxidant Content. American Journal of Biomedical Sciences, 2011; 322-335.
47. Pękal A, Pyrzynska K.. Effect of pH And Metal Ions On DPPH Radical Scavenging Activity Of Tea. International Journal of Food Sciences and Nutrition, 2015; *66*: 58-62.
48. Jiang J, Oberdörster G, Biswas P. Characterization of size, surface charge, and agglomeration state of nanoparticle dispersions for toxicological studies. Journal of Nanoparticle Research, 2008; 11(1): 77-89.
49. Mittal R, Sharma A, Arora S. Ufasomes Mediated Cutaneous Delivery Of Dexamethasone: Formulation And Evaluation Of Anti-Inflammatory Activity By Carrageenan-Induced Rat Paw Edema Model. Journal of Pharmaceutics**,** 2013; 1-12.
50. Agha AM, El-Khatib AS, Al-Zuhair H. Modulation of oxidant status by meloxicam in experimentally induced arthritis. Pharmacol Res., 1999; 40(4): 385–392.
51. Ji C, Sun M, Yu J et al. Trehalose and Tween 80 Improve the Stability of Marine Lysozyme During Freeze-Drying. Biotechnology & Biotechnological Equipment, 2009; 23(3): 1351-1354.